WRF-ARW application to forecasting wind energy, with sensibility of topography.

Alejandro Gutiérrez [a], Gabriel Cazes [b], José Cataldo [c]

[a]*Herrera y Reisig 565, Montevideo, Uruguay, aguti@fing.edu.uy*
[b] *agcm@fing.edu.uy*
[c] *jcataldo@fing.edu.uy*

1INTRODUCTION

As wind power increases its share on the electric systems, it becomes necessary to include short term forecasts in the power dispatch systems (that is, to make optimal choices of the power sources that will be generating electricity within the prediction horizon). The numerical weather forecast allows to predict the wind field in wind farms sites. It should be noted that a significant part of the installed wind farms are placed in sites of complex orography. This makes it necessary to solve the interaction between the large scale flows and the local topography of the farm. Besides this, the interferences of wind turbines within a farm must also be solved.

Currently 30,4 MW of power generation associated to wind energy have been installed in Uruguay. In the next future the wind power generation in Uruguay will increase, and in this scenario, the wind energy forecast will become necessary (Fox, 2007). In this work we advance in the development of prediction tools for the wind energy resource with a forecast horizon of 24 hours (Lange, 2005). The work focus on two topics. One of them is the analysis of numerical simulations obtained with the Weather Research and Forecasting, Advanced Research numerical circulation model (WRF-ARW), version 3.2.1, (Skamarock, 2008) in two different sites, one with a plain, simple topography, and the other with complex topography. In this site it had been installed a wind power farm of 20 MW of nominal power. The second topic consists in the description and validation of a Model Output Statistic (MOS) process that predicts actual power generated by this farm from the WRF-ARW wind forecasts. This MOS aims to account for the interactions of the large scale wind with the local topography and also the wind turbine interferences.

We found that the WRF_ARM has good forecasts skill of wind if the grid resolution is sufficiently high, and that the MOS proposed has god forecasts skill of electric power. The forecast of wind power generation from installed facilities, and from those to be installed will allow to know with less uncertainty the amount of electric energy supplied to the electrical grid from wind power (ANEMOS 2007). The implementation of the MOS in real time operative mode will improve the protocols of electric dispatch.

2WIND MEASUREMENT NETWORK.

The electric public utility of Uruguay (UTE) had installed a wind resource measurement network, with anemometers and wind vanes distributed along the territory of the country. The measurement equipments are NRG cup anemometers NRG # 40 and wind vanes NRG #200P. The system has twenty five measurement stations. In this work we use data from two selected locations of this network to the effects of validating the numerical forecasts obtained from the WRF-ARW. One of these locations is in an area of relatively smooth topography (Pampa station), and the other is located in the site of the wind farm studied, which is placed in an area of relatively complex topography (Fig. 1). In the table 2.1 we present the location and the tower height of these two stations.

Point	Latitude (S)	Lenght (W)	Max Heigh of tower
Caracoles	34°37'	54°57'	67
Pampa	32°14´48,1"	56°12´53,0"	72

Table 2.1 Ubication of the measurement towers.

3WIND FARM STUDIED

A wind farm was installed at the Sierra de los Caracoles. This wind farm is named “Emanuelle Cambilargiu”,and has 10 wind turbines VESTAS V80-2,0 MW. Fig. 3.1 shows the sites of each one of the wind turbines in this farm, and the functioning curve of the VES-TAS V80-2,0 MW wind turbine.

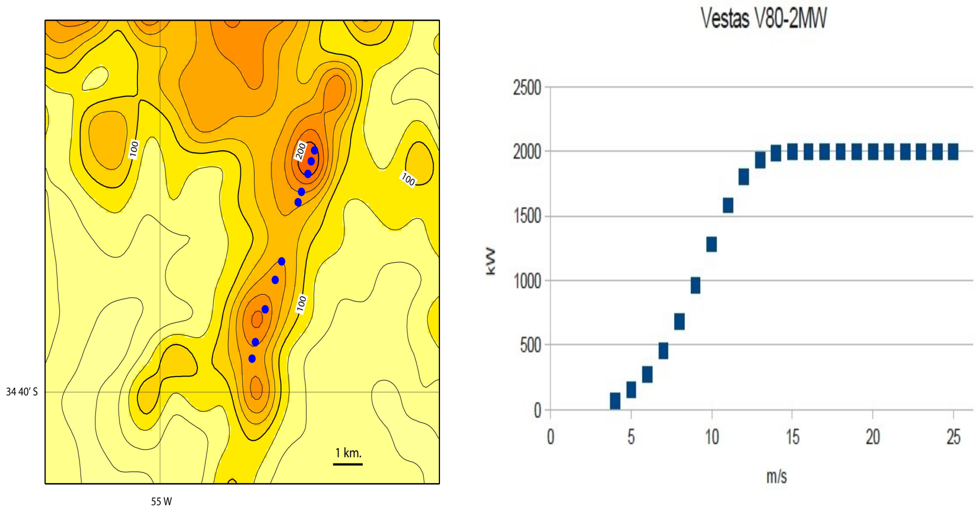

Fig. 3.1. Topography and location of wind turbines at the Emanuelle Cambilargiu wind farm at Sierra Cara-coles (left), and power curve of the VESTAS V80-2.0 MW wind turbine (right).

4WRF-ARW GRIDS AND PARAMETERIZATIONS

The data of the lateral and initial conditions required by the WRF numerical forecasts were obtained from the NOAA Global Forecast System (GFS). The data of the GFS is made publicly available on line in real time by NOAA. The remaining relevant geographical data was downloaded from the WRF-ARW website at the National Center of Atmospheric Research (NCAR), USA. The model was implemented with a two way nested grid, for the domains shown in Fig. 4.1. In the same figure, the topographic features are showed. The horizontal resolutions considered are 30km, 10 km, 3.3 km and 1.1 km. The vertical discretization for all the domains has 28 layers, which span from the Earth's surface to the 30 hPa level. The largest domain (Fig. 3.1 a) includes the location of the two stations presented in the table 2.1, while the other domains (Fig. 3.1 b,c,d) are focused on the Caracoles station. The stations are indicated with blue dots in the figure.

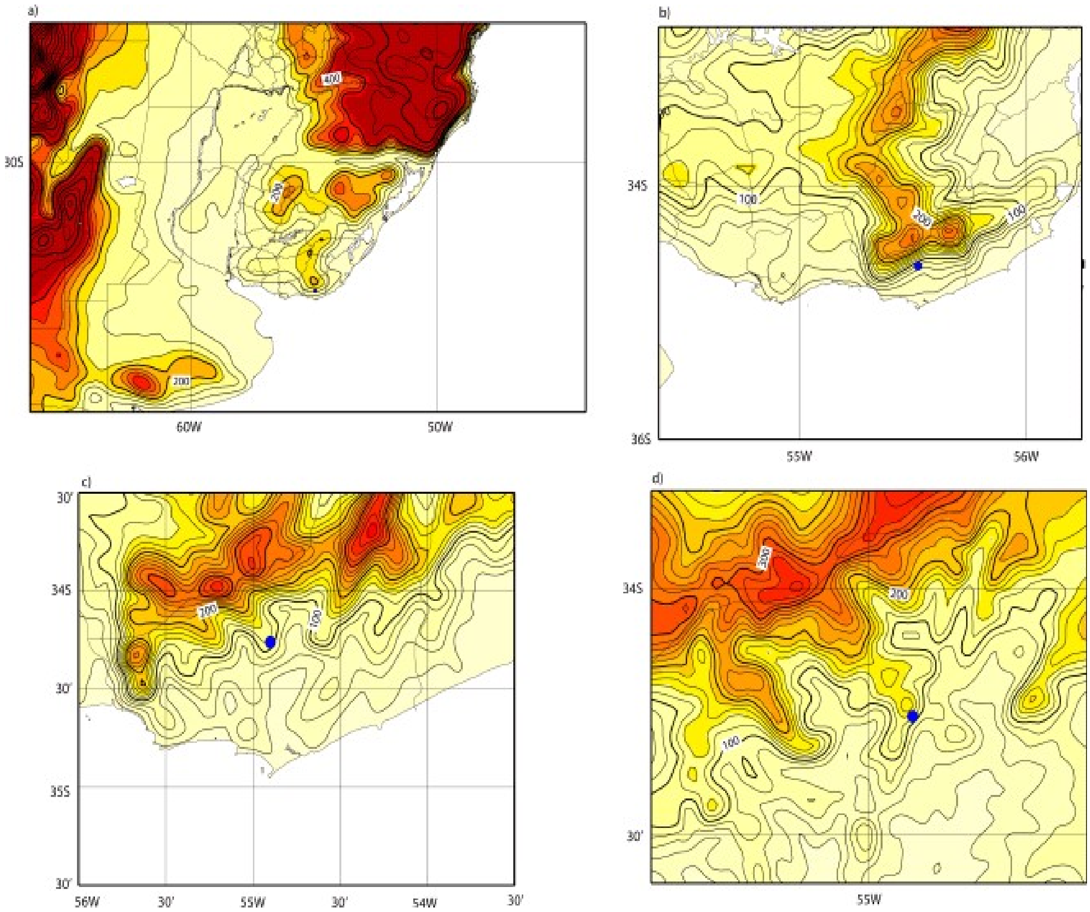

Figure 4.1 Grid nested domains and topography for the implemented domains. a) 30 km b)10 km c)3.3 km d) 1.1km. Pampa and Caracoles stations are indicated with blue dots in a), Caracoles station is indicated with a blue dot in b), c) and d).

WRF dx, dy	Terrain Data set
30 km	10 min
10 km	2 min
3.3 km	30 s
1.1 km	30 s

Table 4.1 Data WRF terrain information and discretization in each grid

The cumulus clouds parameterization used for the first three discretization levels was Kain-Fritshc (Kain and Fritsch 1993). For the last level no cumulus parameterization was used, since its resolution is regarded as cloud resolving. The boundary layer parameterization used for all the discretization levels was the Yonsei University scheme (Hong et al., 2006). This scheme uses a non local K formulation of the turbulent diffusion and an explicit formulation of he PBL top mass entrainment rate. The WRF-ARW was run in the computer cluster of the School of Engineering, Universidad de la República, Uruguay. The forecasts uses the GFS data initialized each day at 12:00 GMT, and extends for 24 hours from 12:00 GMT of the next day after the day of the initialization. It is possible to have the wind power forecast for the indicated period by 21:00 GMT of the initialization day. Forecasts are made available daily at www.fing.edu.uy/cluster/eolica.

5 WIND OBSERVATIONS VS. WIND PREDICTIONS

The WRF-ARW generates forecasts of zonal (West to East) and meridional (South to North) wind components. From these, we compute the wind vector magnitude (in m/s) and the wind direction (in degrees from the North) for each hour of the forecasted period. Figures 5.1 and 5.2 show the validation of the forecasts of wind magnitude (Fig. 5.1) and wind direction (Fig. 5.2) at the Caracoles site during September 2009. The anemometer was not affected by the operation of the wind farm during this month. The forecasts are computed using the results of the domain of 1.1 km horizontal resolution. The forecasted wind is computed at the model grid point closest, both in the horizontal and vertical directions, to the location of the anemometer. We find a relatively good agreement between the observed and forecasted wind magnitude (Fig. 5.1). The agreement between observed and forecasted wind direction (Fig. 5.2) is even better. The MOS to be described in section 5 takes advantage of this fact, since it allows for the correction of systematic forecasts errors that may depend on the wind direction. The domains with lower resolution also show good skill for the forecasts of wind direction, but not for the forecast of wind magnitude (we don't show these results here). This suggests that the relative complexity of the topography at this site make it necessary certain level of resolution to achieve appropriate simulations.

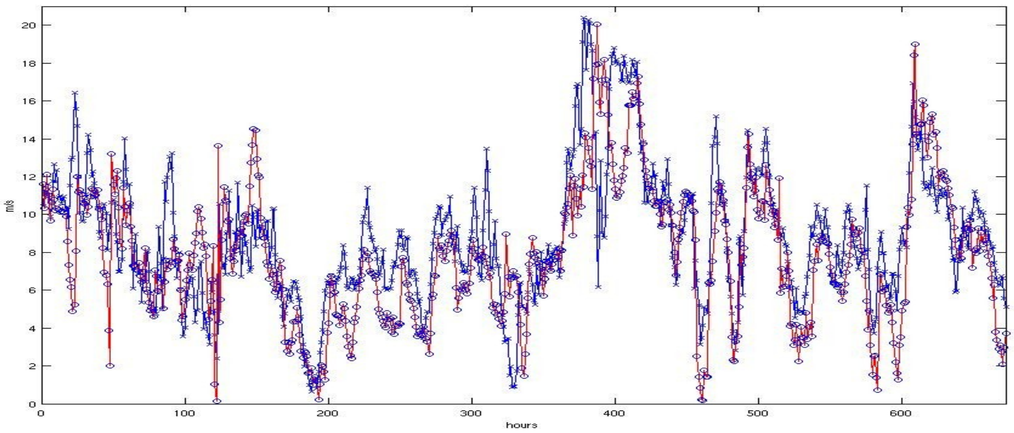

Figure 5.1 (x) measurement of velocity in Caracoles, (o) 24 hours forecast velocity (grid 1.1 km), in m/s.

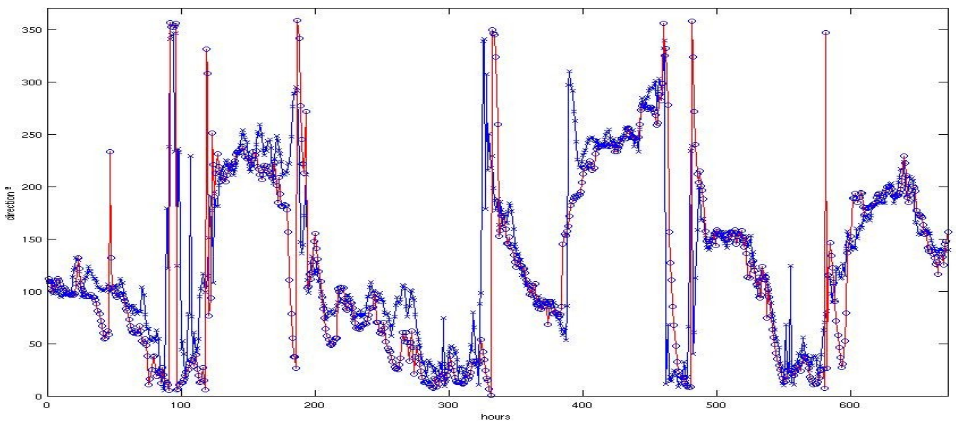

Figure 5.2 (x) measurement of direction in Caracoles, (o) 24 hours forecast direction, in º.

Unlike the Caracoles site, the WRF-ARW forecasts have good skill for Pampa station with the coarse (30km) horizontal resolution. Figure 4.3 show the validation of the forecasts at Pampa site during September 2009 from the 30 km grid.

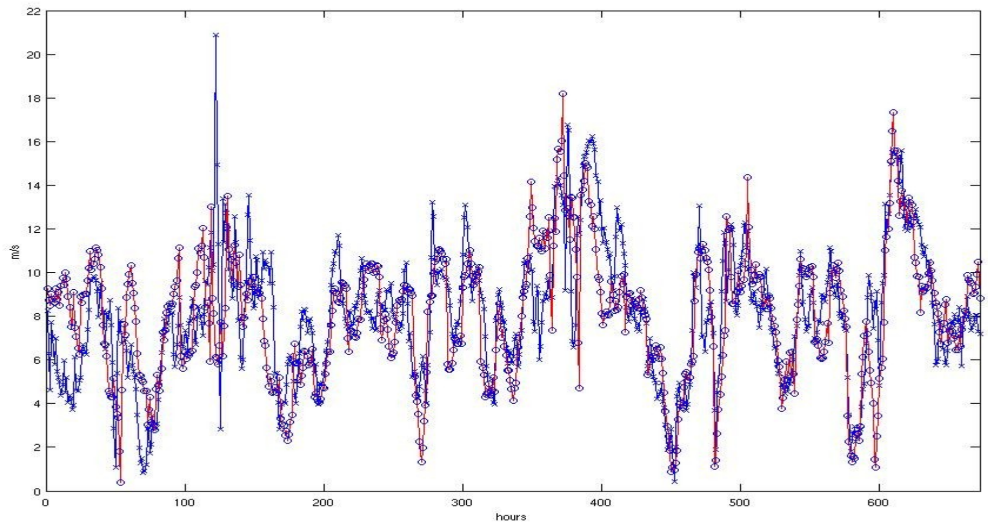

Figure 5.3 (x) measurement of velocity in Pampa, (o) 24 hours forecast velocity (grid 30 km), in m/s.

6DESCRIPTION OF THE MOS

In this section we describe the main aspects of the MOS used for the forecast of electric power of the Emanuele Cambilargiu wind farm. This forecast is computed from the forecasted wind magnitude and direction. Figure 6.1 shows a scheme of the MOS. We define t as the initialization instant of the forecast considered, the forecast of any variable ψ for an instant t+k is defined as ψ(t+k|t).

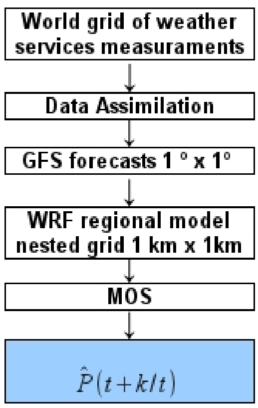

Fig. 6.1. Scheme of the forecasts system.

In sites of complex topography there are sped up factors that depend on the wind direction. Besides this, the interferences among wind turbines also depends on the wind direction. As a consequence it is desirable to propose a MOS that includes the use of the wind direction forecast as an input variable. The development of the MOS is based on the calibration of coefficients that fit a third degree polynomial of the predicted wind magnitude to the generated electric power. These coefficients must depend on the forecasted wind direction, and also on each wind turbine. To this purpose, we divide the wind directions in a set of intervals, and we fit the coefficients for each one of these intervals, and for each one of the wind turbines. We computed the coefficients using data of June, July and August of 2010, while the validation of the MOS and the assessments of its errors are done with data of September 2010 (not used in the calibration process). The time series used were:

–Power generated by each one of the 10 wind turbines installed in the wind farm, $P^i(t+k)$ (i=1,2,...10)

–Wind velocity forecasted in a grid point close to the wind farm, with a horizon of 24 hours, $\hat{V}(t+k/t)$.

–Wind Direction forecasted in the same conditions, $\hat{d}(t+k/t)$.

From the historical series of $P^i(t+k)$, $\hat{V}(t+k/t)$, $\hat{d}(t+k/t)$, we compute the coefficients of Eq. 1, $a_0^i(\hat{d}(t+k/t)), a_1^i(\hat{d}(t+k/t)), a_2^i(\hat{d}(t+k/t)), a_3^i(\hat{d}(t+k/t)),$, in order to minimize the error.

$$\hat{P}^i(t+k/t)=a_0^i(\hat{d}(t+k/t))+a_1^i(\hat{d}(t+k/t))\hat{V}(t+k/t)$$
$$+a_2^i(\hat{d}(t+k/t))\hat{V}^2(t+k/t)+a_3^i(\hat{d}(t+k/t))\hat{V}^3(t+k/t) \qquad \text{(Eq 1)}$$

The total power injected to the electric network by the wind farm is the summ of the power of each wind turbine,

$$P^{windfarm}(t+k/t)=\sum_{i=1}^{i=10} P^i(t+k/t) \qquad \text{(Eq 2)}$$

7VALIDATION OF THE MOS

The MOS was defined considering eighteen intervals of wind directions, each interval has 20º of amplitude. The first interval is [0º,20º], and so on. Figure 7.1 shows the plot of forecasted velocity and power generated for each hour of September 2010. for one of the wind Turbines of the wind farm, and for each direction intervals. The information presented in this figure shows some points with high forecasted velocity and no power generation. These type of cases are associated with no operation of the wind turbine, and hence they were no utilized by the model to calculate the statistical coefficients during the calibration period. However, the validation of the forecast of power during September 2010 don't exclude any data point. The normalized error between the power generated and the forecasted power was calculated for each wind turbine. Figure 7.2 present the normalized error for the wind turbines 1,3,5 and 7.

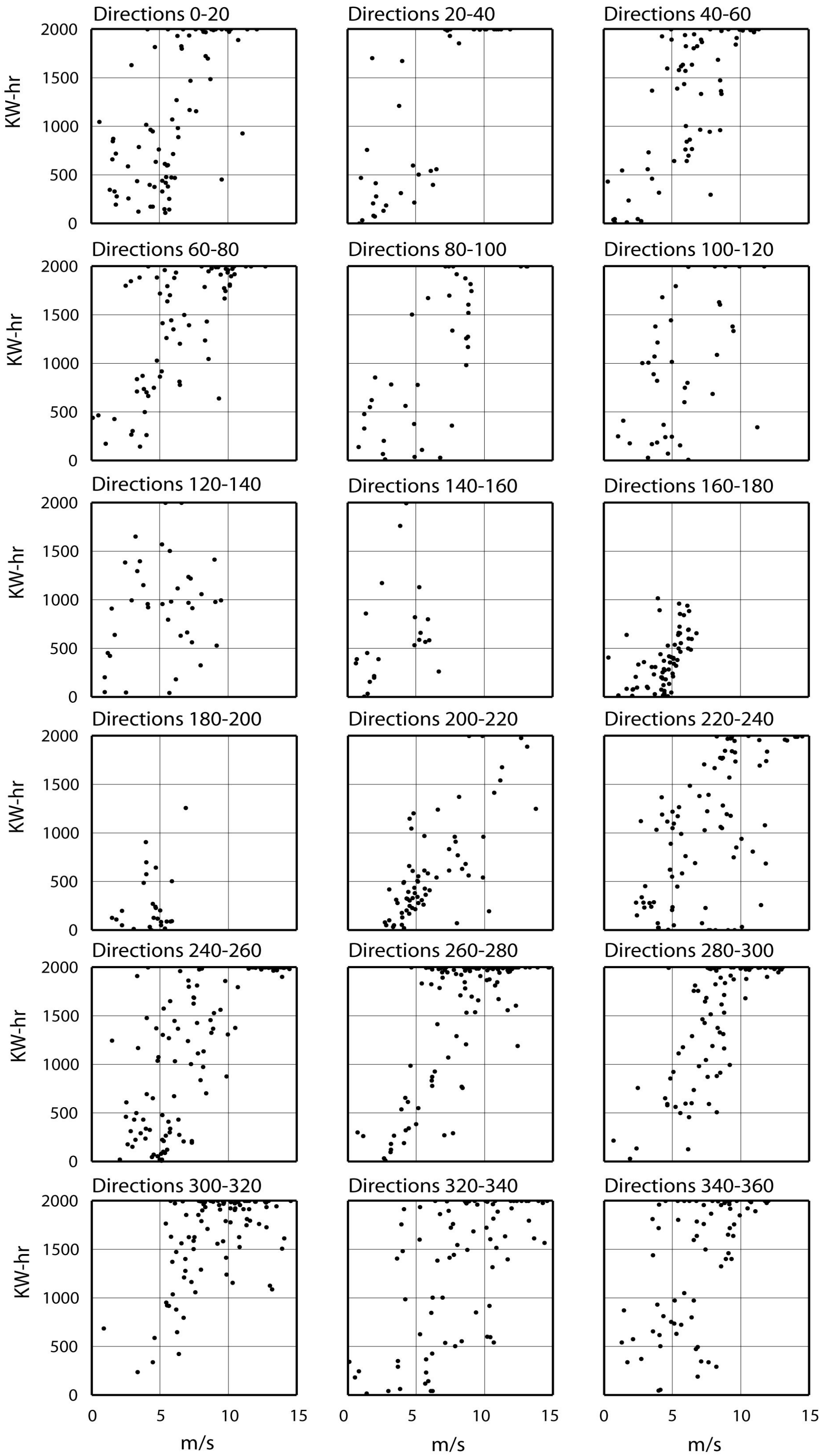

Figure 7.1 For the indicated directions. electric power generated by one of the ten wind turbines installed in the Emanuelle Cambilargiu wind farm (vertical axis) vs. forecasted velocity (horizontal axis), data of September 2010

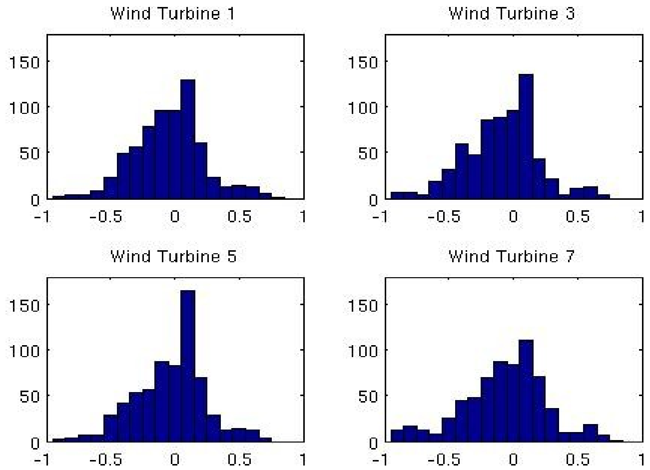

Figure 7.2 Normalized error in the wind power forecasted.

CONCLUSIONS

The forecasts skill of wind direction can be considered as very good in both sites. The forecast of wind magnitude with the 30 km discretization in Pampa (plane site) shows good correlation with the measurements, and hence we conclude it is not necessary to improve the grid resolution. In the Caracoles site, with a complex terrain, the forecast with the nest grid of 1.1 km has good skill, (although slightly than in Pampa). Our hypothesis is that in this case the grid level of discretization was not sufficient to assimilate the terrain affectation of the wind field. Then ,an application of WRF-ARW forecasting in Caracoles may need to improve the simulation by increasing even more the resolution. Currently we are preparing a WRF Large Eddies Simulation (LES), without PBL parameterization and a higher horizontal resolution for the Caracoles site. The MOS showed very encouraging results. The normalized error depends on the wind turbine location.

Aknowledgments: This work was suported by the Agencia Nacional de Investigación e Inovación of Uruguay, ANII. Usinas y Transmisiones del Estado of Uruguay, UTE, cooperated with this work. Computations were done at the Cluster of the School of Engineering, Universidad de la República, Uruguay. Dr. Gabriel Usera of the School of Engineering gave his valuable time assisting with CFD issues. NCAR and NOAA, USA, make available models and forecasts data used in this work.

References

ANEMOS Edición de energía eólica en la UE, Mayo 2007, IDAE, España.

Fox Brendan "Wind Power Integration, Conection and system operatión".The Institutión of Engineering and Technology, United Kingdom, 2007.

Hong, S. Y., Y. Noh and J. Dudhia, (2006): A New Vertical Diffusion Package with an Explicit Treatment of Entrainment Processes. *Mon. Wea. Rev.*, 134, 2318–2341.

Kain, J.S., and J.M. Fritsch, 1993: Convective parameterization for mesoscale models: The Kain- Fritsch scheme. The representation of cumulus convection in numerical models. Meteor. Monogr., No. 24, Amer. Meteor. Soc., 165-170.

Lange, Ulrich Focken, "Physical Aproach to Short-Term Wind Power Prediction" 2005 Springer, Oldenburg, Germany.

Skamarock, June 2008 A Description of the Advanced Research WRF Version 3. NCAR/TN–475+STR NCAR T